ESTIMATING SPACECRAFT ATTITUDE BASED ON IN-ORBIT SENSOR MEASUREMENTS

Kasper Hemme, Britt Jakobsen, Kevin Lyn-Knudsen, Mathias Mølgaard and Michael Nauheimer
Section for Automation and Control, School of Information and Communication Technology,
Department of Electronic Systems, Aalborg University, Denmark
Email: 13gr731@es.aau.dk

***Abstract*—This paper seeks to make an accurate comparison between two different attitude estimation methods: a singular value decomposition (SVD) and an extended kalman filter (EKF). A simulation environment has been constructed using noise parameters obtained both from Earth and from the AAUSAT3 CubeSat currently in orbit. The results have proved that the SVD method is the most accurate of the two methods when sensor noise is low and measurement data is always available. The EKF is more robust against poor sensor data in virtue of using dynamic and kinematic models. However, the EKF is suffering from unmodeled torques, and can be considerably improved when including this in the model. It is apparent from the comparison of noise parameters from Earth and space, that an EKF tuned using Earth measurements of sensor variances will not attain the simulated performance when operated in Low Earth Orbit (LEO). A low estimation error is expected to be attainable by retuning the filter based on space measurement data.**

I. INTRODUCTION

Since the introduction of the CubeSat standard by California Polytechnic State University and Standford University in 1999 [1] the interest in picosatellites has increased exponentially. With the standardized satellite design rules, space has become accessible for low cost satellite missions. CubeSats are generally made with commercial off-the-shelf components to ensure low cost satellites, and because of the standardized CubeSat formfactor, launching of a satellite can be done in the form of piggy-back rides, with the satellite hitching a lift on launch vehicles carrying large commercial satellites. Cheap satellite missions are often linked to university projects, where universities have utilized CubeSats for research and space experiments since 2003 [2], as the low cost and short development time is ideal for university students to participate in the satellite development and operations. However, in recent years commercial and government launched CubeSats are becoming more frequent, and with more advandced CubeSats, the tendency is for CubeSats to be used for commercial operations instead of only research missions.

AAUSAT3 was launched February 2013 as a science experiment for the Danish Maritime Safety Administration, for monitoring ship traffic in arctic regions.

While the mission has been a great success, the matter of attitude determination on-board AAUSAT3 has been minimal at best. Several theoretical methods were designed during the development of the satellite, however, none were implemented on the attitude determination and control system (ADCS) on-board AAUSAT3. With the satellite already in orbit it is possible to collect data directly from space in order to evaluate the performance of different attitude determination methods. In this paper two methods in particular are examined: an SVD [1] method and an EKF [2] method. These methods will have their performance tested using different sensor noise parameters obtained both from a controlled environment on Earth as well as in low earth orbit (LEO). The examination will be performed in a Simulink simulation environment developed for AAUSAT3 [3]. By using noise parameters obtained on Earth as the expected parameters in the determination methods, and simulating the environment using the noise parameters from space, it is possible to assess whether the determination methods can be designed solely on Earth or whether in-orbit tuning/updates of the algorithms are needed.

II. MATERIALS AND METHODS

Attitude of an object in three-dimensional space is described with respect to an inertial reference frame. A reference frame is a right-handed orthogonal Carthesian coordinate system, and the orientation of an object with respect to the inertial frame is the rotation needed to make the inertial frame align with the frame fixed in the object.

The inertial frame used is the Earth Centered Inertial frame (ECI), as defined in [4]. Other frames defined are the Earth Centered Earth Fixed frame (ECEF), the Satellite Body Reference frame (SBRF), both defined in [4], and the Control Reference frame (CRF), which has a fixed orientation with respect to the SBRF, and is defined by the satellite principal axes.

The ECI is convenient in the description of the position of astronomical objects, such as the Sun, with respect to the Earth, while the ECEF is convenient for describing the Earth's magnetic field. Sensor measurements made on the satellite will give vectors described in SBRF, and the attitude of the satellite may be described in either SBRF or CRF, the latter easing satellite dynamics calculations.

A. Attitude Quaternions

A rotation of a vector can be described through a real, isometric matrix left-multiplied with this vector, to obtain its coordinates in the new frame. Alternatively, orientation can be

described in terms of a quaternion. A quaternion is a hyper complex number consisting of a three-dimensional imaginary vector part and a real part. A rotation quaternion is constrained to unit length [5], [6].

$$\mathbf{q} = \mathbf{i}q_1 + \mathbf{j}q_2 + \mathbf{k}q_3 + q_4, \quad ||\mathbf{q}|| = 1 \tag{1}$$

where $\mathbf{q}$ is the quaternion, i, j and k are imaginary entities and q_1-q_4 are the quaternion components.

The relationship between the three imaginary axes defining the vector part of the quaternion, contrary to real axes, is non-commutative.

$$\mathbf{i}^2 = \mathbf{j}^2 = \mathbf{k}^2 = \mathbf{ijk} = -1 \tag{2}$$

$$\mathbf{ij} = \mathbf{k},\ \mathbf{ji} = -\mathbf{k},\ \mathbf{jk} = \mathbf{i},\ \mathbf{kj} = -\mathbf{i},\ \mathbf{ki} = \mathbf{j},\ \mathbf{ik} = -\mathbf{j}$$

The identity quaternion $\mathbf{q} = [0\,0\,0\,1]^T$ equals zero rotation. The inverse of a quaternion is the same as its complex conjugate, and equals the same rotation as the original quaternion but in opposite direction. Sequential rotations are carried out using the non-commutative quaternion multiplication [5]:

$$\mathbf{p} \otimes \mathbf{q} = p_4\mathbf{q}_{1:3} + q_4\mathbf{p}_{1:3} + \mathbf{p}_{1:3} \times \mathbf{q}_{1:3} + p_4q_4 - \mathbf{p}_{1:3} \cdot \mathbf{q}_{1:3} \tag{3}$$

Quaternion multiplication is also used when rotating a vector from one frame into another, augmenting the vector with a zero-valued 4th component, and pre-multiplying with the quaternion conjugate. In this example:

$${}^s\mathbf{v} = {}^s_i\mathbf{q}^* \otimes {}^i\mathbf{v} \otimes {}^s_i\mathbf{q} \tag{4}$$

the vector components in the *s* frame are obtained by rotating the vector given in the *i* frame with the quaternion aligning the *i* frame with the *s* frame.

B. State-Space Model

The general state-space model of the system is

$$\begin{aligned} \dot{\mathbf{x}} &= f(\mathbf{x}, \mathbf{u}) \\ \mathbf{y} &= h(\mathbf{x}, \mathbf{u}) \end{aligned} \tag{5}$$

where $\mathbf{x}$ is the state, $\mathbf{u}$ is the control signal and $\mathbf{y}$ is the measurement vector.

Let the state vector consist of the attitude and the angular velocity of the satellite. The propagation of the attitude part of the state vector is done using the kinematic model for a spacecraft, while the propagation of angular velocity is done using the dynamic model of the satellite.

The kinematic model of the satellite is [5], [6]:

$$\dot{\mathbf{q}}_t = \tfrac{1}{2}[\boldsymbol{\omega}_\otimes]\mathbf{q}_t$$

where

$$[\boldsymbol{\omega}_\otimes] = \begin{bmatrix} [\boldsymbol{\omega}_\times] & \boldsymbol{\omega} \\ -\boldsymbol{\omega}^T & 0 \end{bmatrix}, \quad [\boldsymbol{\omega}_\times] = \begin{bmatrix} 0 & -\omega_3 & \omega_2 \\ \omega_3 & 0 & -\omega_1 \\ -\omega_2 & \omega_1 & 0 \end{bmatrix} \tag{6}$$

The dynamic model of the satellite (in the CRF frame) is [6]:

$$\dot{\boldsymbol{\omega}}_t = {}^c\underline{\mathbf{J}}^{-1}({}^c\underline{\mathbf{J}}\boldsymbol{\omega}_t \times \boldsymbol{\omega}_t + \boldsymbol{\tau}_{\text{ctrl},t})$$

The prediction of the measurement vector is made using orbit parameter data propagated through an ephemeris model and through a model of the Earth magnetic field to obtain the sun and magnetic field vectors, respectively. The gyroscope prediction is equal to the predicted angular velocity.

C. Attitude Estimation Using SVD

The SVD method is a single-frame method, i.e. it estimates the attitude based on measurements from a single time step only. The SVD method, like almost any point method used for attitude determination, determines the attitude by seeking the optimal solution to Wahba's problem, which is defined by the minimization of the cost function:

$$J(\underline{\mathbf{R}}) = \sum_{i=1}^{n} a_i \left\| \mathbf{b}_i - \underline{\mathbf{R}}\mathbf{r}_i \right\|^2, \qquad n \geq 2 \tag{7}$$

where $\mathbf{b}$ and $\mathbf{r}$ are the measurement vector in the rotating frame and the model propagated vector in the inertial reference frame, respectively, and $\underline{\mathbf{R}}$ is the optimal rotation matrix for all sets of vectors (in this case the sun and magnetic field vectors).

According to [7] the minimization of the cost function is equivalent to the maximization of the function:

$$trace(\underline{\mathbf{R}}\mathbf{B}^T) \tag{8}$$

where

$$\underline{\mathbf{B}} = \sum_{i=1}^{n} a_i \mathbf{b}_i \mathbf{r}_i^T \tag{9}$$

with a_i, a weighing parameter determined by expected sensor accuracy. The singular value decomposition of the matrix $\underline{\mathbf{B}}$:

$$\underline{\mathbf{B}} = \underline{\mathbf{U}}\underline{\mathbf{\Sigma}}\underline{\mathbf{V}}^T = \underline{\mathbf{U}}\, diag[\Sigma_{11}\, \Sigma_{22}\, \Sigma_{33}]\underline{\mathbf{V}}^T \tag{10}$$

will give the optimal rotation matrix $\underline{\mathbf{R}}_{\text{opt}}$ through the following relation [7]:

$$\underline{\mathbf{R}}_{\text{opt}} = \underline{\mathbf{U}}[1 \quad 1 \quad det(\underline{\mathbf{U}})det(\underline{\mathbf{V}})]\underline{\mathbf{V}}^T \tag{11}$$

This rotation matrix can be converted into a quaternion as defined in [5].

D. Attitude Estimation Using EKF

The Extended Kalman filter is a recursive filter, i.e. it estimates the attitude based on the latest measurement along with the previous attitude estimate. In the a priori predict step it estimates the present state $\mathbf{x}_k$ and measurement vector $\mathbf{y}_k$, and the state transition covariance $\underline{\mathbf{P}}$ based on the previous state $\mathbf{x}_{k-1}$ and state transition covariance [8]:

$$\begin{aligned} \hat{\mathbf{x}}_{k|k-1} &= f(\hat{\mathbf{x}}_{k-1}, \mathbf{u}_k) \\ \hat{\mathbf{y}}_{k|k-1} &= h(\hat{\mathbf{x}}_{k-1}) \\ \underline{\mathbf{P}}_{k|k-1} &= \underline{\mathbf{\Phi}}_k \underline{\mathbf{P}}_{k-1} \underline{\mathbf{\Phi}}_k^T + \underline{\mathbf{Q}}_k \end{aligned} \tag{12}$$

The function f is implemented as a Runge-Kutta approximation of the discrete-time propagation of the state [6]:

$$\begin{aligned}\dot{\mathbf{x}} &= f(\mathbf{x}) \\ k_1 &= f(\mathbf{x}_k) \\ k_2 &= f(\mathbf{x}_k + \tfrac{1}{2}T_s k_1) \\ k_3 &= f(\mathbf{x}_k + \tfrac{1}{2}T_s k_2) \\ k_4 &= f(\mathbf{x}_k + T_s k_3) \\ \mathbf{x}_{k+1} &= \mathbf{x}_k + \tfrac{1}{6}T_s(k_1 + 2k_2 + 2k_3 + k_4) \end{aligned} \tag{13}$$

The $\underline{\mathbf{\Phi}}$ and $\underline{\mathbf{H}}$ matrices are transition matrices employing system dynamics and models of sensor data, respectively:

$$\underline{\mathbf{\Phi}} = \underline{\mathbf{I}}_7 + T_s \begin{bmatrix} \frac{1}{2}\dfrac{\partial f_{\text{kin}}}{\partial \mathbf{q}} & \frac{1}{2}\dfrac{\partial f_{\text{kin}}}{\partial \boldsymbol{\omega}} \\ \underline{\mathbf{0}}_{3\times 4} & \dfrac{\partial f_{\text{dyn}}}{\partial \boldsymbol{\omega}} \end{bmatrix} \qquad \underline{\mathbf{H}} = \begin{bmatrix} \dfrac{\partial\, {}^c\mathbf{v}_{\text{sun}}}{\partial\, {}^c_i\mathbf{q}} & \underline{\mathbf{0}}_{3\times 3} \\ \dfrac{\partial\, {}^c\mathbf{v}_{\text{mag}}}{\partial\, {}^c_i\mathbf{q}} & \underline{\mathbf{0}}_{3\times 3} \\ \underline{\mathbf{0}}_{3\times 4} & \underline{\mathbf{I}}_3 \end{bmatrix}$$

The function h is implemented as the matrix $\underline{\mathbf{H}}$ times the a priori estimate of the state. The matrix $\underline{\mathbf{Q}}$ is a tuning parameter comprising the covariance matrix of the state transition noise.

The a posteriori step of the Kalman filter updates the state and the state transition matrix, based on the Kalman gain $\underline{\mathbf{K}}$:

$$\begin{aligned}\underline{\mathbf{K}}_k &= \underline{\mathbf{P}}_{k|k-1}\underline{\mathbf{H}}_k^T(\underline{\mathbf{H}}_k\underline{\mathbf{P}}_{k|k-1}\underline{\mathbf{H}}_k^T + \underline{\mathbf{R}}_k)^{-1} \\ \hat{\mathbf{x}}_k &= \hat{\mathbf{x}}_{k|k-1} + \underline{\mathbf{K}}_k(\mathbf{y}_k - \hat{\mathbf{y}}_{k|k-1}) \\ \underline{\mathbf{P}}_k &= (\underline{\mathbf{I}} - \underline{\mathbf{K}}_k\underline{\mathbf{H}}_k)\underline{\mathbf{P}}_{k|k-1} \end{aligned} \tag{14}$$

where $\underline{\mathbf{R}}$ is the measurement noise covariance matrix.

For faster convergence of the Kalman filter, the SVD method is used for the first time instance in order to obtain an initial estimate of the state vector, while the state transition covariance matrix is guesstimated on basis of the assumed accuracy of the satellite dynamic model.

E. Simulink Simulation Environment

A Simulink simulation environment developed for AAUSAT3 is used to test the two attitude estimation methods. The environment contains a continuous-time "truth model" which the estimations are compared to in order to determine the estimation error. Additionally the environment contains models of each of the sensors on AAUSAT3 and finally the on-board software of the satellite.

The "truth model" uses the orbital parameters of AAUSAT3 contained in the Two Line Element (TLE) including orbit altitude (780 km) and inclination (98.55°) along with a specification of time. Three models are used with the orbital parameters and time as inputs. To obtain the position of the satellite in the ECI frame, the 4th order Simplified General Perturbations (SGP4) model is used. The position is used with the International Geomagnetic Reference Field (IGRF) to model the Earth's magnetic field in the ECEF. An Ephemeris model gives the position of the sun in the ECI frame. The "truth model" also comprises a continuous-time model of the spacecraft kinematics and dynamics along with spacecraft parameters, including dimensions (0.10x0.10x0.11 m), mass (0.958 kg) and inertia matrix. Finally the "truth model" simulates environmental disturbance torques from atmospheric drag, solar radiation and magnetic residuals, along with the torque resulting from the permanent magnet on AAUSAT3.

The sensor models contain the sampling time, bias and calculated variances for each of the sensors. For the first test of the estimation methods the Earth measured variances are applied, for the second the space measured variances are applied.

The on-board software comprises, apart from the SVD and the EKF, the same models for propagation of the estimated measurement vector as the "truth model", i.e. the SGP4, IGRF and Ephemeris, along with TLE data. In the EKF the initial state guess is an arbitrary quaternion and an angular velocity close to the expected two revolutions per orbit (0.1°/s) for the detumbled satellite. The $\underline{\mathbf{P}}$ matrix is initialized with an identity matrix multiplied with an arbitrary constant. The matrix $\underline{\mathbf{R}}$ contains the sensor noise variances from the Earth measurement in both simulations, and $\underline{\mathbf{Q}}$ is tuned to obtain the smallest possible error in the case where the sensor model contains the Earth measured variances.

F. Sensor Noise Type and Covariance Matrix

In order to realistically assess the performance of the employed estimation methods, the sensor noise type and covariance matrix have to be determined for each sensor.

With AAUSAT3 currently in orbit, it is possible to estimate the noise parameters from the sensors both in a controlled environment on the surface of the Earth, as well as in Low Earth Orbit (LEO).

By using both sets of data, it is possible to determine whether a measurement of noise levels performed on Earth is sufficient for spaceflight attitude estimation, or whether it is preferred to update the noise parameters during spaceflight.

To estimate the noise parameters, two measurement sessions have been performed, measuring the sensor inputs over a prolonged period of time. The first session is a static sensor test in a controlled environment on the surface of the Earth. The second session consists of in-orbit measurements on AAUSAT3.

The static sensor session on Earth is performed with the satellite stationarily placed in a controlled magnetic field with a static light source, and measuring the sensor inputs with a sampling frequency of 1 Hz during a period of 18 hours.

The in-orbit sensor session is performed by logging sensor measurements on AAUSAT3 with a frequency of 1 Hz over a period of 6 hours. While this session was running, no radio uplink was established to AAUSAT3.

The sample autocorrelation function (ACF) together with the power spectral density (PSD) are used to identify the type of noise on each sensor input. When the noise types are identified, the covariance matrices for all the sensors are determined. The ACF and covariance matrices will be calculated using the functions shown in equation 15 and 16, respectively.

$$R_{xx}(j) = \frac{1}{N}\sum_{n=0}^{N-1} x_n x_{n-j} \tag{15}$$

where R_{xx} is the autocorrelation of x.

$$\Sigma_{\mathbf{XY}} = \mathrm{E}[(\mathbf{X} - \mathrm{E}[\mathbf{X}]) \cdot (\mathbf{Y} - \mathrm{E}[\mathbf{Y}])^{\mathrm{T}}] \tag{16}$$

where $\Sigma_{\mathbf{XY}}$ is the covariance matrix of the vectors $\mathbf{X}$ and $\mathbf{Y}$.

III. Results

A. Analyzing Noise on Ground and in Orbit

Measurements have been made on the sun sensors, magnetometers and gyroscope on Earth and in space in order to analyze the noise that is present on the signals. In the Earth measurements, the sensors were placed in a static magnetic field in front of a static light source. In space, the measurements were performed with a varying magnetic field and light source. Figure 1a shows the x-axis of the in-orbit measurements from the magnetometer. To be able to analyze the noise on this signal, several local high order Taylor approximations have been made and subtracted from the measured signals, to leave only the noise as shown in figure 1b. From analyzing the ACF and PSD of the sensor noise signals, it is seen that the noise appears to be white for all the sensors; see an example in figure 1c. This also means that the noise can be modeled as a Gaussian random process. The covariance matrices of a Gaussian random process can be calculated as shown in equation 16, and the covariance matrices for the sensor noise are as given below, with e and s denoting Earth and space measurements, respectively.

$$\Sigma_{sun,\,e} = \begin{bmatrix} 96.30 & 0.8360 & -17.91 \\ 0.8360 & 1.401 & 6.931 \\ -17.91 & 6.931 & 39.56 \end{bmatrix} \cdot 10^{-6} \tag{17}$$

$$\Sigma_{sun,\,s} = \begin{bmatrix} 1076 & -84.99 & -492.9 \\ -84.99 & 757.1 & 67.49 \\ -492.9 & 67.49 & 758.5 \end{bmatrix} \cdot 10^{-6} \tag{18}$$

$$\Sigma_{mag,\,e} = \begin{bmatrix} 0.4099 & 0.0188 & -0.1979 \\ 0.0188 & 0.4215 & -0.2737 \\ -0.1979 & -0.2737 & 0.2620 \end{bmatrix} \cdot 10^{-6} \tag{19}$$

$$\Sigma_{mag,\,s} = \begin{bmatrix} 67.53 & -1.665 & 9.074 \\ -1.665 & 59.30 & 0.7495 \\ 9.074 & 0.7495 & 41.61 \end{bmatrix} \cdot 10^{-6} \tag{20}$$

$$\Sigma_{gyro,\,e} = \begin{bmatrix} 1839 & 168.3 & 107.1 \\ 168.3 & 2765 & -585.6 \\ 107.1 & -585.6 & 3934 \end{bmatrix} \cdot 10^{-6} \tag{21}$$

$$\Sigma_{gyro,\,s} = \begin{bmatrix} 140860 & 29178 & 40170 \\ 29178 & 135527 & 45550 \\ 40170 & 45550 & 253840 \end{bmatrix} \cdot 10^{-6} \tag{22}$$

Note that the covariance matrix of the gyroscope noise is given in proportion to the sampled values, while that of the magnetometer and sun vector matrices are given for the normalized vectors.

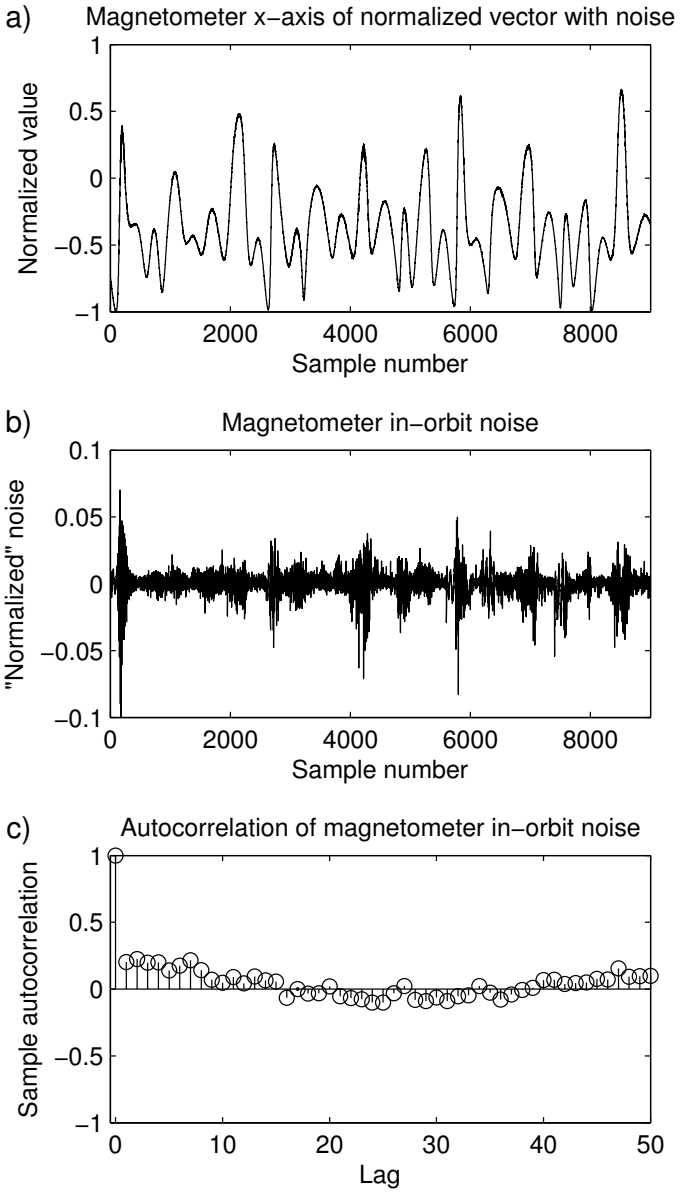

Fig. 1. The top graph shows the x-axis of sampled and normalized magnetometer vector. The graph in the middle shows only the noise of the signal. The bottom graph shows the ACF of the noise.

From the covariance matrices it is seen, that the covariance of the noise on the sun vector measured in space is more than 100 times larger than that off the measurements from Earth. The same thing is seen for the magnetometer. For the gyroscope it is in the area of 50 times larger for the space measurements than for those from Earth.

B. Attitude Estimation Results

The results of the attitude estimation performance have been obtained with the following noise covariance matrix $\underline{\mathbf{R}}$, process noise covariance matrix $\underline{\mathbf{Q}}$ and initial error covariance

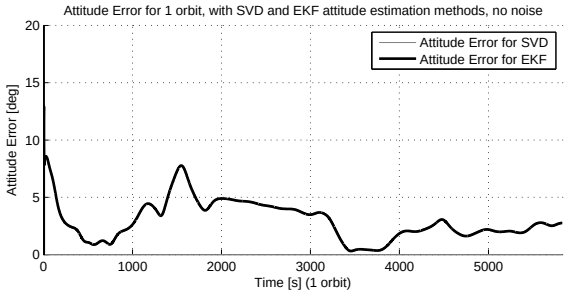

Fig. 2. Simulation of attitude estimation error of the SVD and the EKF without sensor noise.

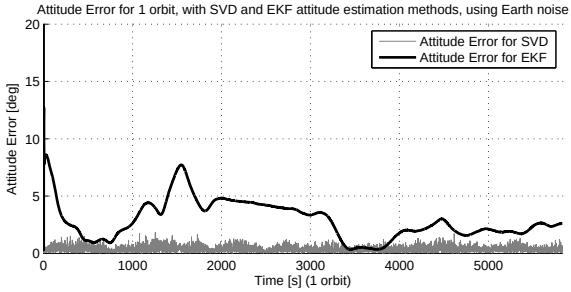

Fig. 3. Simulation of attitude estimation error of the SVD and the EKF with sensor noise from Earth measurements.

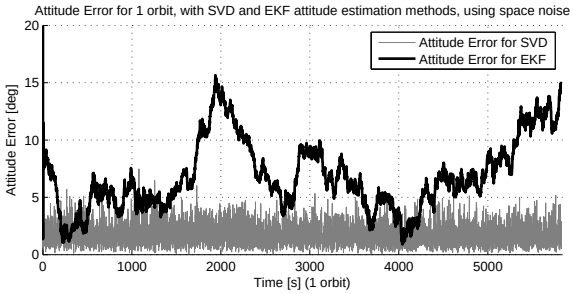

Fig. 4. Simulation of attitude estimation error of the SVD and the EKF with sensor noise from space measurements.

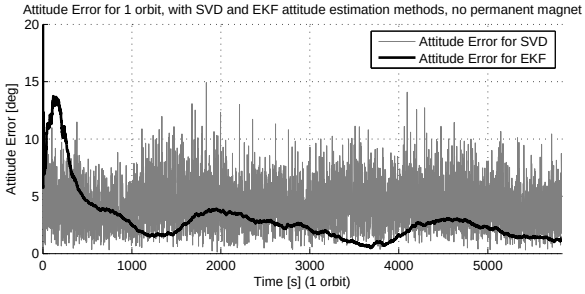

Fig. 5. Simulation of attitude estimation error of the SVD and the EKF with increased sensor noise and without a permanent magnet on the satellite.

matrix $\underline{\mathbf{P}}_0$ for the EKF and with equal weights for the SVD method.

$$\begin{aligned}\underline{\mathbf{R}} &= [96.30\,1.401\,39.46\,1\,0.409\,0.421 \\ &\quad 0.262\,1\,1839\,2765\,3934] \cdot 10^{-6} \\ \underline{\mathbf{Q}} &= [5 \cdot 10^{-14}\,5 \cdot 10^{-14}\,5 \cdot 10^{-14}\,5 \cdot 10^{-14}\,100\,5\,1] \\ \underline{\mathbf{P}}_0 &= [0.001\,0.001\,0.001\,0.001\,0.001\,0.001\,0.001] \cdot 10^{-3}\end{aligned} \tag{23}$$

An attitude estimation error is found using the "truth model" and calculating the difference between the true attitude and the estimated attitude. All simulations are made with environmental disturbances torques modeled for AAUSAT3 orbit, at 780 km altitude. In the first three simulations a permanent magnet is included in the "truth model", which causes an addisional disturbances torque.

A simulation length of approximately one orbit (5830 s) without sensor noise is shown in figure 2. The SVD estimation method has no attitude estimation error, while the EKF method shows an estimation error of up to 7.7°, and an average estimation error of 2.8°.

A simulation with the sensor noise measured on Earth prior to launch is shown in figure 3. Here the SVD estimation method has an estimation error of up to 1.8° and an average estimation error of 0.3°, while the EKF method again shows an estimation error of up to 7.7°, and an average estimation error of 2.8°, i.e. an average error about 4 times larger than that of the SVD, and a maximum error about 9 times larger.

A simulation with the sensor noise measured in space is shown in figure 4. Here the SVD estimation method has an estimation error of up to 7.4° and an average estimation error of 1.7°, while the EKF method shows an estimation error of up to 15.6°, and an average estimation error of 6.8°, i.e. an average error about 2 times larger than that of the SVD, and a maximum error about 4 times larger.

Finally figure 5 shows a simulation excluding the permanent magnet and with the sensor noise further increased to the levels used in previous work on AAUSAT3 attitude estimation [9]. The noise is added as a Gaussian noise for the sun vector, magnetic field vector and the angular rate with a standard deviation of 3.33°, 3° and 0.2° respctively. In this simulation the SVD estimation method has an estimation error of up to 14.9° and an average estimation error of 4.2°. Disregarding the first 1000 samples, the EKF method shows an estimation error of up to 3.9°, and an average estimation error of 2.1°, i.e. an average error about 4 times smaller than that of the SVD, and a maximum error about 2 times smaller.

IV. Discussion

The SVD method proves to have the best attitude estimation accuracy for the measured satellite sensor noise, its maximum error being approximately half that of the EKF when subjected to the space noise. It is expected that the deficiency of the EKF is due to the inaccuracy of the EKF dynamic model, which does not include the permanent magnet. This is also indicated by figure 5.

Adding sensor noise generally affects the accuracy of SVD method more than that of the EKF, which is seen from the difference in the simulation shown in figure 2 with no noise, to the simulation shown in figure 3 with the pre-orbit measured noise. It is evident that the EKF attitude error does not increase, while the SVD attitude error is increased from

0° to 1.8°. While still outperforming the EKF method, this confirms the SVD to be more sensitive to the sensor noise increase.

Looking at the measurements of the noise on the sensors from space, compared to that of the measurements from Earth, it is seen that the covariance matrices of for the space noise are considerably larger. This is the result of using commercial-off-the-shelf components and not space-graded components.

When subjected to the larger space noise, as seen in figure 4, both the SVD and EKF estimate errors have increased, the SVD by a factor of 4 and the EKF only by a factor of 2. In this test case the EKF noise covariance matrix $\underline{\mathbf{R}}$ does not match the sensor noise variances, and the process noise covariance matrix $\underline{\mathbf{Q}}$ has not been re-tuned for the variances used in the updated sensor model.

Because of the unmodeled permanent magnet torque and the sensor noise covariance matrix $\underline{\mathbf{R}}$ no longer being correct, the EKF becomes less reliable. As the EKF is relying on the measured angular velocity to propagate the satellite kinematics and in turn obtain an attitude estimate, the increased variance for the angular rate measurement is greatly influencing the overall performance of the EKF.

The main problem for the EKF is the requirement for accurate models for satellite dynamics and kinematics, control- and disturbance torques, but also for the process noise and sensor noise. As the simulations in figure 2, 3 and 4 are made with an unmodeled permanent magnet torque, unknown disturbance torques as well as having a sun synchronous orbit, they are biased in favor of the SVD.

Removing the permanent magnet from the simulations and increasing the sensor noise, yields another result as shown in figure 5. The EKF performs better as the system model used in the EKF is more accurate, and the EKF attitude error considerably smaller than that of the SVD.

Further development would be to include the permanent magnet in the dynamic model of the EKF. To obtain a better foundation for final conclusions, Monte Carlo simulations should be conducted, perturbing different parameters, e.g. TLE time initialization or initial angular velocity, to investigate which of the methods are more robust. Finally all simulations should also be run with eclipse cycles.

ACKNOWLEDGMENT

The authors would like to thank the AAUSAT3 Team: Hans Peter Mortensen, Troels Jessen, Jeppe Ledet-Pedersen, Jesper Knorr Larsen and Kasper Vinther.

REFERENCES

[1] J. Puig-Suari and B. Twiggs, *CubeSat Design Specification*, rev 12. California Polytechnic State University, 2009.

[2] L. Alminde et al., *Educational Value and Lessons Learned from the AAU-Cubesat Project*, Institute of Electrical and Electronics Engineers, 2003.

[3] R. Amini et al. *Design and Implementation of a Space Environment Simulation Toolbox for Small Satellites*, IAC-05-E2.3.06. 56th International Astronautical Congress, 2005.

[4] J. R. Wertz and W. J. Larson, *Space mission analysis and design*, 3rd ed. Space Technology Library, 1999.

[5] M. J. Sidi, *Spacecraft dynamics & control - a practical engineering approach*, no. 7. Press Syndicate of the University of Cambridge, 1997.

[6] J. R. Wertz, *Spacecraft attitude determination and control*. D. Reidel Publishing Company, 1978.

[7] F. L. Markley and D. Mortari, *How to estimate attitude from vector observations*, AAS Paper 99-427. NASA, 1999.

[8] M. S. Grewal and A. P. Andrews, *Kalman filtering theory and practice using MATLAB*, 2nd ed. John Wiley Interscience, 2001.

[9] K. Vinther et al. *Inexpensive CubeSat Attitude Estimation Using Quaternoins and Unscented Kalman Filtering* 2010.